Optimizing Reflection and Orientation for Bifacial Photovoltaic Modules

A Thesis

Presented in Partial Fulfillment of the Requirements for Graduation with Distinction in the Department Mechanical Engineering at The Ohio State University

By

Raymond Dong

The Ohio State University

2009

Examination Committee:

Mark Walter, Advisor

Gary Kinzel

Approved by:

____

Department of Mechanical Engineering

Table of Contents

1 Abstract

Currently, the world market for photovoltaic (PV) solar panel technology is expanding rapidly. The increasing market for PV panels reflects the increasing demand for a clean, reliable energy solution and indicates that PV panels may be the method of choice for supplementing today's global energy needs. Although PV solar panel production is rising, PV panels are still a relatively new and high-priced technology. There remains a need for a commercially-viable method of implementing residential-scale photovoltaic systems for consumer homes.

The purpose of this study is to ultimately maximize the irradiance (solar radiation energy) incident on a geometrically constrained 6.84-kilowatt photovoltaic array system, and thereby maximize the energy production. In this study, the optimum height and angle of bifacial (two-sided) PV modules are investigated both analytically and experimentally. Analytical methods utilize the sun's position and average irradiance throughout the course of a day. Data is collected under actual, outdoor sunlight conditions. Furthermore, stationary flat reflectors with specular (mirror-like) and diffuse (light-scattering) reflection are used to experimentally characterize the amount of sunlight directed on the back face of the PV modules.

By validating the theoretical results with experimental evidence, the analytical model can be used to accurately predict the optimum orientation and reflective material for any location and time of year. The findings suggest that a diffusely scattering reflector is a cost-efficient solution for the proposed PV array design.

2 Project Overview

2.1 Introduction

Interest in clean and renewable energy sources is growing and will continue to grow as more people recognize that fossil fuels like coal, oil, and natural gas are limited resources and that burning fossil fuels releases large amounts of carbon dioxide, a greenhouse gas, into the Earth's atmosphere. Renewable energy sources are derived from everyday occurrences in the environment, from items that can be re-grown, or from bi-products of human/animal activity (National Renewable Energy Laboratory, 2008). The most prominent and environmentally benign forms of sustainable energy are captured from natural sources like wind, ocean tides, and sunlight.

Among the many renewable energy alternatives, solar energy remains one of the most well-known and adaptable methods for producing heat and electricity. For smaller, residential-scale applications, solar energy is used to heat water or is converted directly to electricity through photovoltaic (PV) solar panels. For larger, utility-scale applications, solar energy can feed vast PV solar panel farms, or be concentrated to vaporize fluids or to run heat engines.

Today, the United States Department of Energy is working to develop cost-competitive solar energy systems by spending more than $170 million annually in research and development on concentrated solar power (CSP) and photovoltaic technologies (U.S. Department of Energy, 2008). Increasing energy reliability, promoting economic growth, and reducing carbon emissions are the desired benefits that stem from the development of cost-competitive solar energy systems.

2.2 Solar Decathlon

The 2009 U.S. Department of Energy Solar Decathlon is a competition between twenty teams of students, from colleges and universities across the globe. Contending teams are challenged to design and build an attractive, energy-efficient house that is powered entirely by the sun. The competition is sponsored by the U.S. Department of Energy and will be held in October in Washington, D.C. More information can be found at www.solardecathlon.org.

The Solar Decathlon is named for its ten scored contests (U.S. Department of Energy, 2008) as shown in Table 1.

Table 1: Ten contests for the 2009 U.S. Department of Energy Solar Decathlon competition.

#	Contest	Points	Scoring
1	Architecture	100	subjective
2	Engineering	100	subjective
3	Market Viability	100	subjective
4	Lighting Design	75	subjective
5	Communications	75	subjective
6	Comfort Zone	100	objective
7	Hot Water	100	objective
8	Appliances	100	objective
9	Home Entertainment	100	objective
10	Net Metering	150	objective

Table 1 shows that five of the contests are scored subjectively while the other five contests are scored objectively. Attractiveness, viability, and ease of operation are judged and scored subjectively, whereas maintaining temperature and humidity, providing hot water, and running home appliances are evaluated objectively.

Perhaps the most significant contest is "Net Metering" in which the goal is to produce more electricity than is consumed during competition week. While all houses are grid-tied, meaning that electricity can be drawn at any time from a main electrical grid, excess electrical power that is produced by the house can also be fed back into the main grid. Two meters will monitor incoming and outgoing power. A net zero energy balance is required for 100 of the contest's points, bonus points are awarded when the house generates more electricity than is consumed.

In association with the Ohio State University Solar Decathlon Team, this study aims to maximize the efficiency of the rooftop photovoltaic array in order to meet the energy requirements of the competition. Table 2 charts the electrical loads of all power consuming appliances in the OSU Solar Decathlon house, based on the functional requirements of the competition schedule.

Table 2: Estimated Power Consumption for the Solar Decathlon competition week.

Mechanical Equipment	Brand	Model #	Power Consumption [kW]	Run Time [hours]	Times Used	Energy Consumption [kW-h]
Washer	Whirlpool	WFC7500C	0.37	1	10	3.65
Dryer	Whirlpool	LDR3822P	0.25	1	10	2.49
Cooktop	Wolfe	CT15I/S	1.70	2	6	20.40
Surface Exhaust	Gaggenau	VL 040/041-707	0.25	2	4	2.00
Oven	Whirlpool	GH7208XR	1.35	1	2	2.70
Dishwasher	KitchenAid	KUDD03ST	1.44	2	7	20.13
Television	Toshiba	42XV545U	0.18	80	1	14.40
Audio Equipment	Yamaha	YSP – 4000	0.12	50.5	1	6.06
Refrigerator	Whirlpool	ET5WSEXV	0.16	24	8	30.72
Computer	HP	Compaq dc7900	0.14	40	1	5.40
Home Automation	BuildingLogix	JACE-2 w/ IO-34	0.01	24	8	1.63
Lights - general	GE	Ultra T5	0.60	18	8	86.40
Lights - task	GE	CFL	0.30	43	1	12.90
Temp. Sensor	Yamatake	TY7321	0.00	24	8	0.06
Humidity Sensor	Yamatake	HTY7033	0.00	24	8	0.14
Daylight Sensor	LightSaver	LS – 301	0.00	24	8	0.14
Contact Sensor	Smart Home	SM-204	0.01	0.5	1	0.01
PoU Water Heater	EEMax	EX190	19.00	2	1	38.00
ERV	Fantech	VHR704	0.40	12	8	38.40
Hot Water Heat Pump	Etech	R106K5	1.20	4	8	38.40
Circulating Pump	Taco	00R-IFC	0.03	12	8	2.86
Split System AC	Mitsubishi	MSZ-A12NA	0.00	0	0	0.00
Total Energy Consumption [kW-h]						**326.9**

Table 2 shows that the estimated total energy consumption for the weeklong competition is approximately 327 kW-h. This value is nearly twice as large as what the team would expect from typical, commercially available PV panels. The predicted energy deficiency is just one source of motivation for this research project.

2.3 Bifacial Photovoltaic Modules

The employment of bifacial photovoltaic modules is one innovative feature of the PV array design. In particular, the PV modules are 190-watt Hit Double panels made by Sanyo Electric Co. These modules not only collect sunlight from the front panel face, but as illustrated in Figure 1, they also collect sunlight from the back panel face using ambient light reflected off of surrounding surfaces. This ability to harvest solar energy from the back face thus increases the electricity generation per module area.

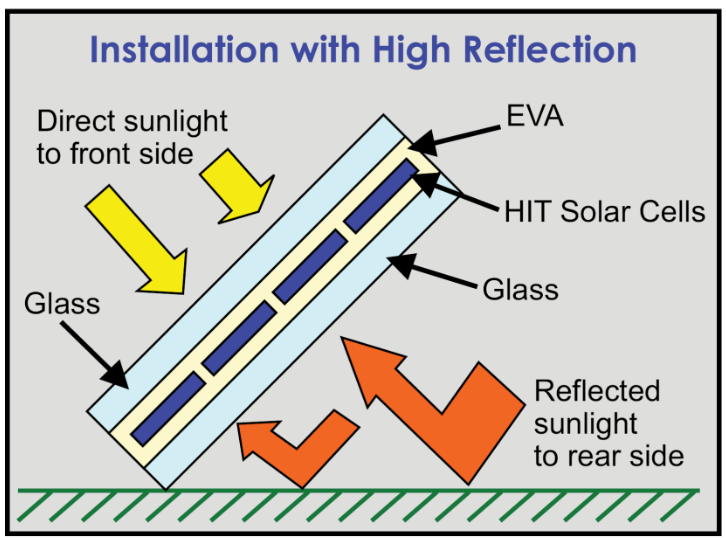

Figure 1: Backside harvesting of bifacial PV module (Sanyo Electric Co., 2008).

The Sanyo panels are rated at 190W under Standard Test Conditions (STC) for the front panel face alone (Sanyo Electric Co., 2008). In addition, Sanyo claims that up to 30% more electrical power can be generated by the Hit Double panels than conventional monofacial (one-sided) photovoltaic modules. The electrical specifications, including backside irradiation, are presented on the data sheet in Appendix section 9.1.

2.4 Stationary Flat Reflectors

Another means for increasing the bifacial PV panel efficiency per module area is to amplify the amount of sunlight incident on the back side of the PV panel by adding a stationary reflective surface directly beneath the bifacial PV panel, as illustrated in Figure 1. Sanyo recommends that no mirrors or lenses be used to focus or concentrate sunlight on the Hit Double panels (Sanyo Electric Co., 2008). Parabolic reflectors that concentrate sunlight often cause high local irradiance and cell temperatures that result in panel power losses (Hall, Roos, & Karlsson, 2005). The increase in cell temperature with increased irradiance is one major difficulty associated with application of reflective materials to PV panel systems. Past research has demonstrated that the efficiency of crystalline silicon PV modules decrease as the temperature increases by approximately 0.4 – 0.5 %/°C (Ronnelid, Karlson, Krohn, & Wennerberg, 2000).

According to Ronnelid *et al.*, cell temperature and irradiance distribution on a PV panel are of vital importance to the performance of the panel (Ronnelid, Karlson, Krohn, & Wennerberg, 2000). Having uniform irradiance is especially important for PV modules with crystalline silicon cells, but is less important for thin-film PV modules. Although the individual solar cells in both crystalline PV and thin-film PV are wired in series, thin-film PV modules demonstrate higher acceptance of uneven illumination.

Ronnelid *et al.*'s study in Sweden showed that stationary, flat reflectors mounted at the front of monofacial PV modules had increased the annual output of the module by an order of 20 – 25% (Ronnelid, Karlson, Krohn, & Wennerberg, 2000). As illustrated in Figure 2, the annual output further improved with increased reflector width and with increased number of yearly adjustments to the reflector tilt angle.

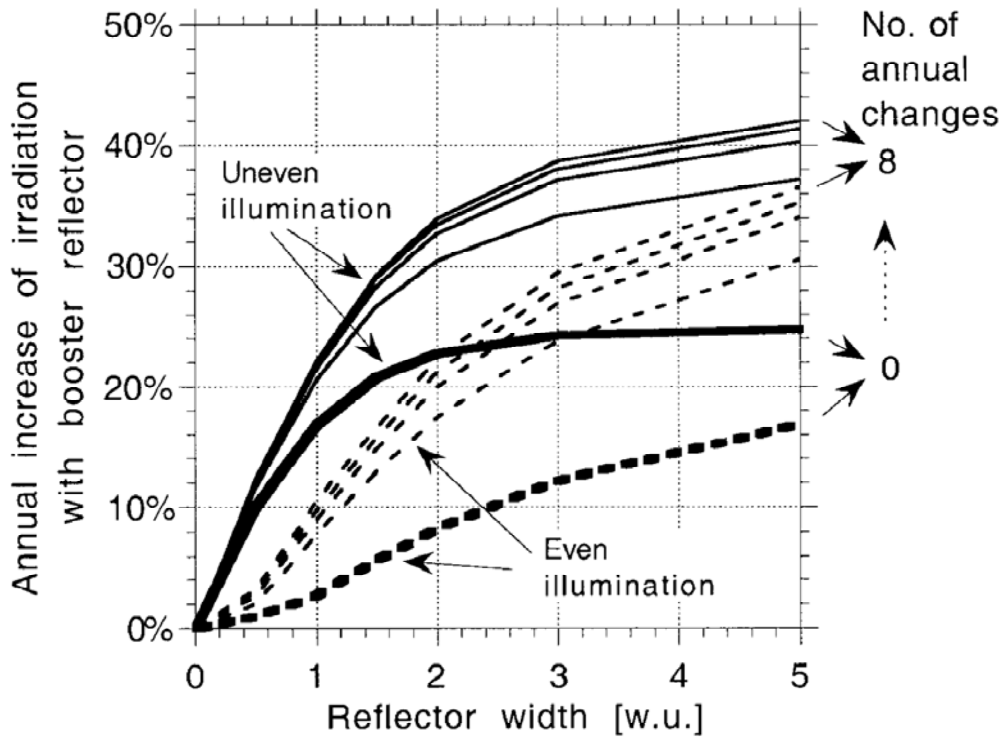

Figure 2: Annual increase of irradiation onto PV modules versus reflector width (with respect to PV module width) when the reflector tilt is changed 0, 2, 4, 6, and 8 times annually. The reflector is assumed to be specular with ρ = 0.8. The PV module is assumed to be south-facing. (Ronnelid, Karlson, Krohn, & Wennerberg, 2000)

The reason for adjusting the tilt of the reflector is to maximize the amount of sunlight directed normal to the PV panel face, and thereby increase the power generated by the PV panel. Since the sun's path across the sky changes throughout the year, the reflector is adjusted accordingly to increase the solar radiation that is hitting the panel. The bold lines in Figure 2 are for reflectors that are kept stationary for the entire year. The solid lines are for PV modules that accept uneven irradiation (*i.e.*, thin-film PV); whereas the dotted lines are for PV modules that only accept even irradiation (*i.e.*, crystalline silicon PV). This plot demonstrates that with either type of photovoltaic panels, the use of low-cost reflectors causes a significant increase in solar radiation incident on a given PV module, and hence the power output of the PV panel is also increased.

2.5 Effects of Shading

Because of the way silicon-based PV panels function, shading of a solar panel can degrade the panel performance by much more than just the loss of one shaded module. Since PV panels consist of strings of solar cells connected in series, the cell producing the smallest current (receiving the least irradiance) hinders the overall power output. Current generated from other cells is forced to flow through the shaded cells, causing reverse-voltages across the cells and undesirable heating to occur (Sanyo Electric Co., 2009). This explains why crystalline silicon PV modules are sensitive to uneven illumination. The most poorly illuminated cell governs the PV module output; whereas the other solar cells, experiencing higher irradiance, cause adverse heating that diminishes the module efficiency. Figure 3 illustrates a series-connected PV module and different scenarios where the module is partially shaded.

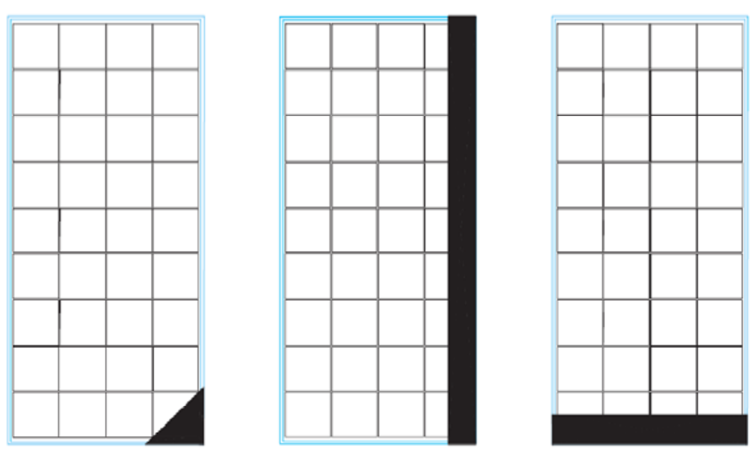

Figure 3: Examples of partial-cell shading that reduce PV module power output by ½ (Kyocera Solar, Inc., 2004).

The reduction in PV module power output is proportional to the area shaded for any one solar cell or any string of cells (Kyocera Solar, Inc., 2004). As illustrated in Figure 3, shading half of one cell or half of a string of cells reduces the power output by 50%.

In some cases, PV modules like the Sanyo Hit Double have built-in bypass diodes that navigate current around the weaker cells that are partially shaded and generating less electricity. The bypass diodes minimize undesirable heating and current reduction (Sanyo Electric Co., 2009). In any case, shading obstructions like fences, pipes, chimneys, tree branches, and other PV modules should be avoided whenever possible.

2.6 Problem and Purpose

In association with the 2009 Ohio State University Solar Decathlon Team, this research investigates design parameters associated with a 6.84-kilowatt photovoltaic (PV) array system to be mounted on the rooftop of an 800 square-foot house. Figure 4 shows a computer-aided depiction of the Solar Decathlon house with 36 photovoltaic modules in the rooftop array. The modules in the PV array face south all year round but are able to adjust to different tilt angles so as to optimize irradiance (solar radiation energy) directed normal to the PV panel faces.

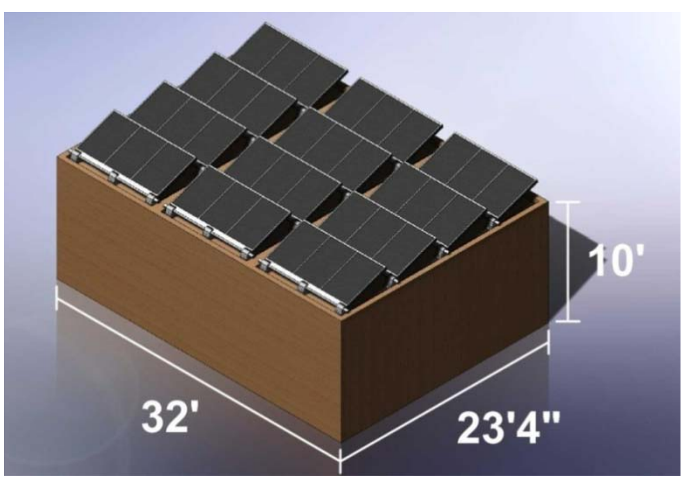

Figure 4: Solar Decathlon house with rooftop photovoltaic array.

The purpose of this study is to maximize the solar irradiance that is hitting the photovoltaic array, and thereby maximize the energy production. Given the limited area on the rooftop, bifacial (two-sided) photovoltaic (PV) modules are implemented in order to enhance electricity production per module area. However, the optimum height above the roof and optimum angle for these bifacial PV modules are unknown. Additionally, stationary flat reflectors are employed to amplify the amount of sunlight directed on the back face of the PV modules. There is currently no information on which type of reflector surface profile will yield the best PV module performance.

2.7 Objectives

The major objectives of this research project are:

- To study the performance of bifacial photovoltaic modules and its dependence on:
    1. flat, stationary, low-concentrating reflectors
    2. solar panel elevation above the reflector material
    3. solar panel tilt
- To determine the optimum PV module tilt angle and elevation for the October, 2009 Solar Decathlon competition to be held in Washington, D.C.
- To determine the flat reflector surface profile – whether specular (mirror-like) or diffuse (light-scattering) – yielding the best PV module performance.

2.8 Approach to Achieving the Objectives

The plan of action for this research project was divided into two major parts. The first part involved theoretical investigations with analytical methods that can predict the optimum PV module tilt angle for the 2009 Solar Decathlon competition. The second part of this research study involved experimental investigations with outdoor testing of PV modules. After evaluating the results of these two investigations, conclusions were made about the validity of the analytical findings, as verified by experimental evidence. Further conclusions were made about the optimum reflection and orientation of the proposed Solar Decathlon Team's PV array design.

3 Theoretical Investigations

3.1 Methodology for Theoretical Analysis

The theoretical investigations were approached in two different ways. The first approach involved writing a MATLAB program to compute discrete values of PV array power output throughout the course of one day, based on sun angles and incoming solar irradiance. Though described as a manual, interpolation method, the MATLAB program is used to evaluate the PV module performance in Washington, D.C. for any particular day of interest and for varying degrees of tilt. The MATLAB code for this manual, interpolation method is shown in Appendix section 9.2.

The second approach in the theoretical analysis involved an online solar performance calculator called PVWATTS ver.2, developed by the National Renewable Energy Laboratory (NREL). The PVWATTS program was a useful tool for quickly computing PV module performance in Washington, D.C. for all twelve months of the year and for varying degrees of tilt. The PVWATTS solar calculator was used to determine the credibility of the MATLAB code developed in the first approach.

3.2 Sun Angles

Knowledge of the sun's position in the sky is fundamental to understanding PV panel performance. The two angles of importance are solar azimuth and solar altitude, as illustrated in Figure 5.

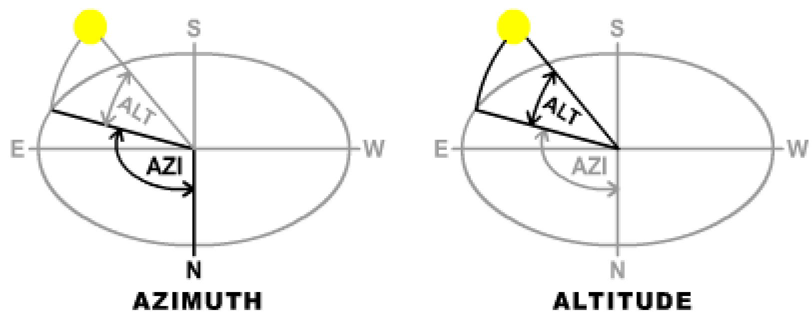

Figure 5: Sun's position in the sky given as azimuth and altitude angles (Autodesk, Inc., 2008).

Solar azimuth characterizes the sun's angle on the horizontal plane, relative to true north. When viewed from above, the azimuth angle is always a positive value measured in a clock-wise direction from true north (Autodesk, Inc., 2008). Solar altitude characterizes the sun's vertical angle, relative to the horizontal ground plane. Altogether, azimuth and altitude angles express the path of the sun as it rises from the East and falls to the West throughout the course of one day. It is important to note that the sun's position is dependent on the geographical location (*i.e.*, latitude and longitude) of a particular site.

While the sun's position continually changes throughout the course of one day, it also varies seasonally throughout the course of a year. Figure 6 illustrates how the sun's path differs between the summer and winter solstices. The summer and winter paths are distinctly different for both azimuth and altitude angles. Figure 6 demonstrates that the sun's altitude is relatively high in the sky during the summer as compared to the winter. This seasonal change of the sun's path greatly influences the optimum PV module tilt for any particular time of year.

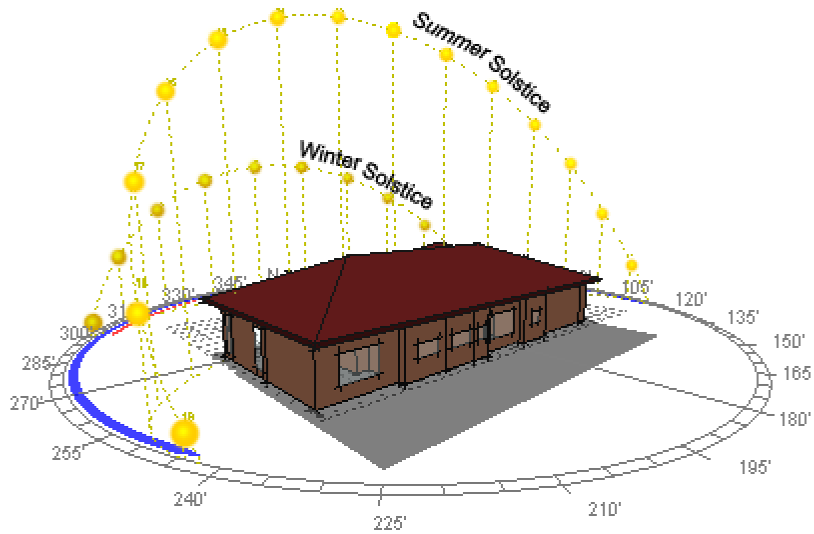

Figure 6: Sun's path through the sky in summer and winter (Autodesk, Inc., 2008).

3.3 Insolation

Solar insolation is another piece of knowledge vital to understanding PV panel performance. Derived from "incident solar radiation", insolation is a measure of electromagnetic (solar radiation) energy incident on a given area at a given time (Wikipedia, 2009). Generally, insolation is expressed as average irradiance in units of watts per square meter (W/m2) or kilowatt-hours per square meter per day (kW-h/m2/day). As with the sun's position, solar insolation continually changes throughout the day, and throughout the course of a year. Insolation varies not only with time; it is dependent on geographical location, climate, air quality, and atmosphere (*i.e.*, cloud cover). Figure 7 shows the average insolation across the United States during the month of June.

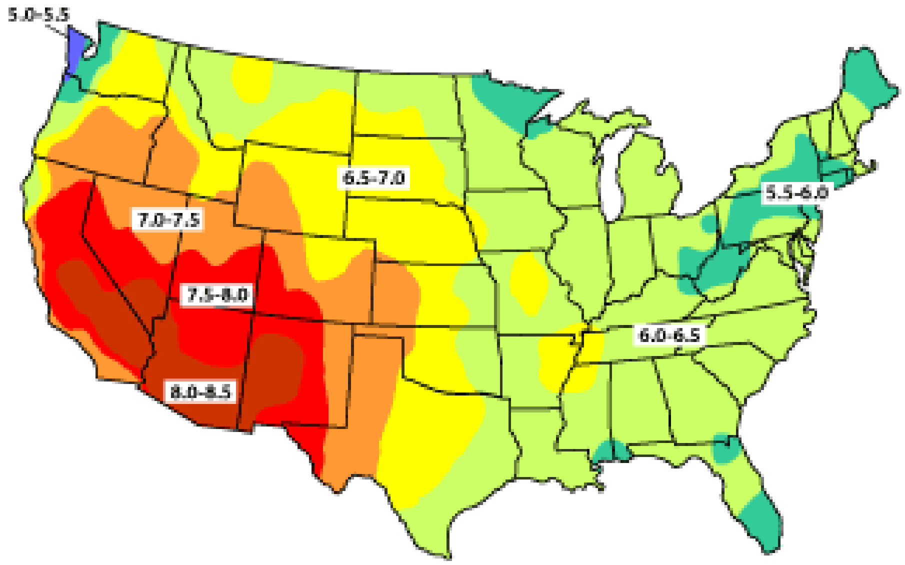

Figure 7: Average insolation on a horizontal surface across the continental United States in the month of June, expressed in units of kW-h/m^2/day (U.S. Department of Energy, 2008).

Figure 7 illustrates that the Southwest region of the U.S., depicted in red, receives relatively high insolation as compared to the Midwest states like Ohio. This explains why most solar energy installments, including concentrated solar power plants and PV solar farms, exist in the Southwest United States. Regardless of the comparatively low insolation, it is still feasible to develop solar energy systems in Ohio. Despite having lower average annual insolation than Ohio, Germany is the world's leading PV installer with a total capacity of over 3,830 megawatts as of 2007 (Wikipedia, 2009).

One important distinction about solar insolation is how the sun's radiation reaches the earth's surface. Direct insolation refers to the unobstructed solar irradiance that comes straight from the sun, whereas diffuse insolation refers to the solar irradiance that is reflected or scattered by clouds, dust, and other air particles in the earth's atmosphere (U.S. Department of Energy, 2008). Global insolation refers to the total radiation, the summation of direct and diffuse components of sunlight, incident on a given surface element. As illustrated in Figure 8, PV modules make use of direct sunlight, as well as diffuse sunlight reflected off of clouds, the ground, and other surrounding surfaces.

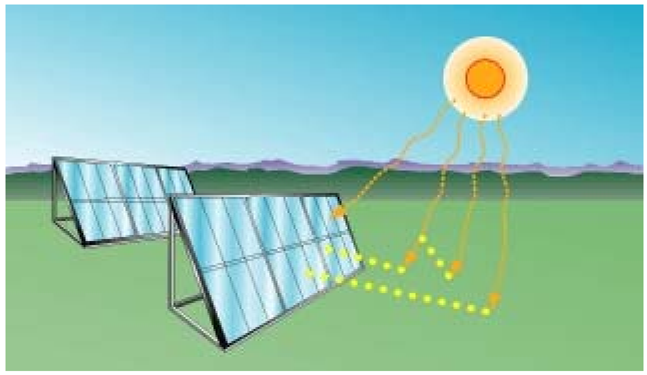

Figure 8: PV modules receiving direct and diffuse sunlight.

3.4 MATLAB Code

Given knowledge of sun angles, insolation, and PV module efficiency, the expected power output for a 6.84 kW PV array can be computed. The azimuth and altitude angles are obtained from an online solar position calculator developed by the National Oceanic and Atmospheric Administration (NOAA, 2009). Input parameters for the NOAA calculator are time, date, and location (*i.e.*, latitude and longitude coordinates). Values for monthly direct insolation in Washington, D.C., averaged over a 22-year period, were obtained from solar insolation data tables developed by the National Aeronautics and Space Administration (NASA, 2009).

Table 3 shows a summary of sun angles and direct irradiance values for October 12th, 2009. This table shows only a small portion of data (from 7:00am to 9:00am) that was collected for the entire day.

Table 3: Summary of sun angles and direct solar radiation for October 12th, 2009 (NASA, 2009).

Time of day	Minutes from midnight	Sun Angles Altitude (°)	Sun Angles Azimuth (°)	Direct Irradiance (W/m^2)
(Sunrise) 7:17	437	0.1	80.6	0.0
7:30	450	2.4	78.6	7.5
7:45	465	5.1	76.2	15.7
8:00	480	7.9	73.7	23.5
8:15	495	10.6	71.2	31.0
8:30	510	13.3	68.7	38.0
8:45	525	16.0	66.0	44.7
9:00	540	18.6	63.3	51.0

For Table 3, irradiance was assumed to climax at midday and to decrease to zero at sunrise and sunset. A quadratic curve fit was used to interpolate values for direct irradiance, as shown in Figure 9. For this elementary analysis, diffuse irradiance was not considered.

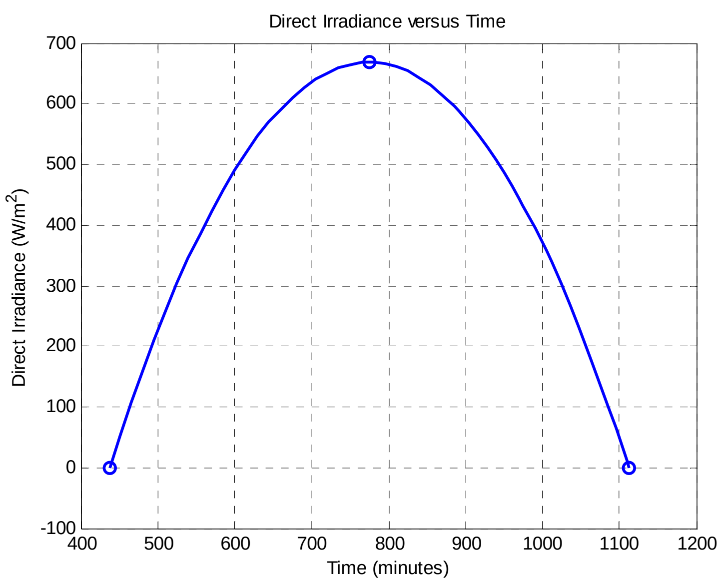

Figure 9: Approximated irradiance curve, using quadratic fit, for the duration of one day. The peak insolation value was based on a 22-year average. The abscissa represents time of day expressed in minutes, where midnight is the 0th minute.

Using basic geometry, the magnitude of direct solar radiation perpendicular to the front face of a given PV module was calculated. This computation occurred in two distinct steps. Figure 10 illustrates the geometry for the first step, whereas Figure 11 illustrates the second step.

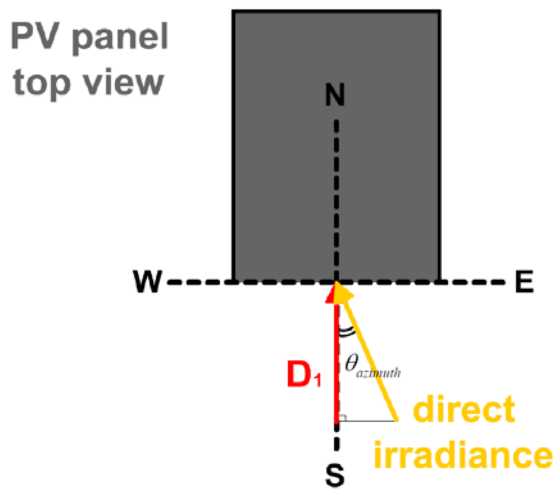

Figure 10: Top view of PV module.

Viewing the PV module from above as shown in Figure 10, the magnitude of direct irradiance projected onto the south-facing plane was calculated as follows:

$$D_1 = (direct\ irradiance) \cdot \cos(\theta_{azimuth}) \tag{4.1}$$

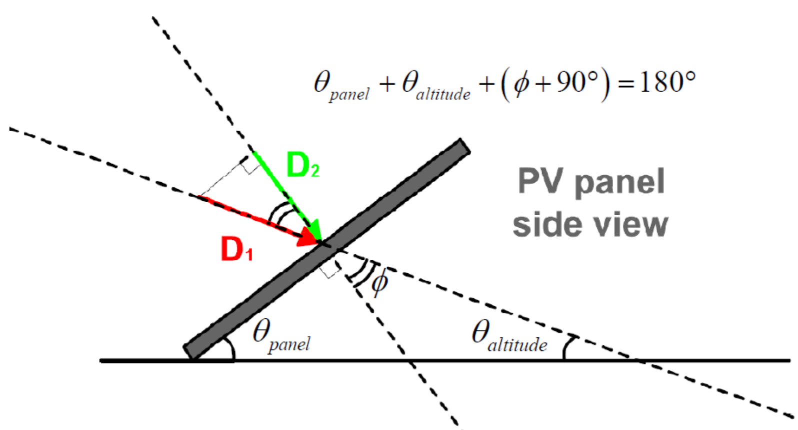

Figure 11: Side view of PV module.

Then, viewing the PV module from the side as shown in Figure 11, the magnitude of direct irradiance perpendicular to the front face of the PV module was calculated as follows:

$$\phi = 90° - \theta_{panel} - \theta_{altitude} \tag{4.2}$$

$$D_2 = D_1 \cos(\phi) \tag{4.3}$$

After computing the amount of direct solar radiation incident on the face of the PV module, the estimated power output was calculated for varying PV panel tilt angles, ranging from 0° to 90°. The PV panel efficiency was assumed to be 15.7% (Sanyo Electric Co., 2008). The results showed that for the week of the 2009 Solar Decathlon competition in Washington, D.C, the optimum PV panel tilt angle is 54°. Figure 12 plots the estimated power output for a single, monofacial (one-sided) PV module throughout the duration of one day. Note that a *monofacial* PV module is assumed, because the solar energy harvested from the back face of a bifacial PV module is unknown.

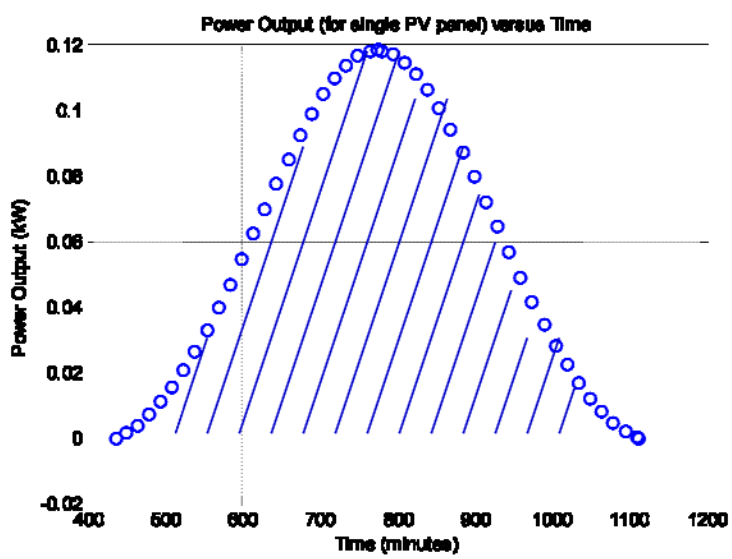

Figure 12: Estimated power output for a single south-facing, monofacial, 190-watt PV module in Washington, D.C. throughout the course of one day in October, 2009 based on a 22-year average. The abscissa represents time of day expressed in minutes, where midnight is the 0th minute.

As illustrated in Figure 12, the area under the curve was computed to find the total energy production for the entire day. For a 6.84-kilowatt array with south-facing, monofacial PV panels tilted at 54°, the estimated energy output for the week of competition in Washington, D.C. is calculated to be 215 kW-h. Note that the estimated output falls short of the estimated total energy consumption given in Table 2.

3.5 PVWATTS Performance Calculator

The PVWATTS performance calculator is an online tool used to quickly estimate the monthly energy output of any PV array. PVWATTS uses hourly weather data for a "typical meteorological year" for locations all across the United States (NREL, 2009). Figure 13 shows the input parameters for the specified PV system, including site location, size of the PV array, tilt of the PV array, and whether the PV array is fixed or tracking. Figure 13 also shows the resulting monthly energy output for the specified PV system.

PVWatts

AC Energy & Cost Savings

Cautions for Interpreting the Results

Station Identification	
Cell ID:	0263376
State:	Maryland
Latitude:	38.8 ° N
Longitude:	76.9 ° W
PV System Specifications	
DC Rating:	6.84 kW
DC to AC Derate Factor:	0.810
AC Rating:	5.54 kW
Array Type:	Fixed Tilt
Array Tilt:	0.0 °
Array Azimuth:	180.0 °
Energy Specifications	
Cost of Electricity:	8.2 ¢/kWh

Results			
Month	Solar Radiation ($kWh/m^2/day$)	AC Energy (kWh)	Energy Value ($)
1	2.07	331	27.07
2	2.79	424	34.67
3	4.19	702	57.40
4	5.03	792	64.76
5	5.70	895	73.18
6	6.16	925	75.64
7	5.82	886	72.45
8	5.18	792	64.76
9	4.39	661	54.05
10	3.35	529	43.26
11	2.21	332	27.15
12	1.89	286	23.39
Year	4.07	7556	617.85

Figure 13: PVWATTS performance calculator, demonstrating input specifications and resulting energy production estimates for Washington, D.C. (NREL, 2009).

As with the MATLAB analysis, PVWATTS computed the estimated performance for the specified 6.84 kW PV array at vary tilt angles, ranging from 0° to 90°. Using both MATLAB and PVWATTS computation methods, Figure 14 provides the estimated energy output for 36 south-facing, monofacial, 190-watt PV modules during the week of competition in Washington, D.C..

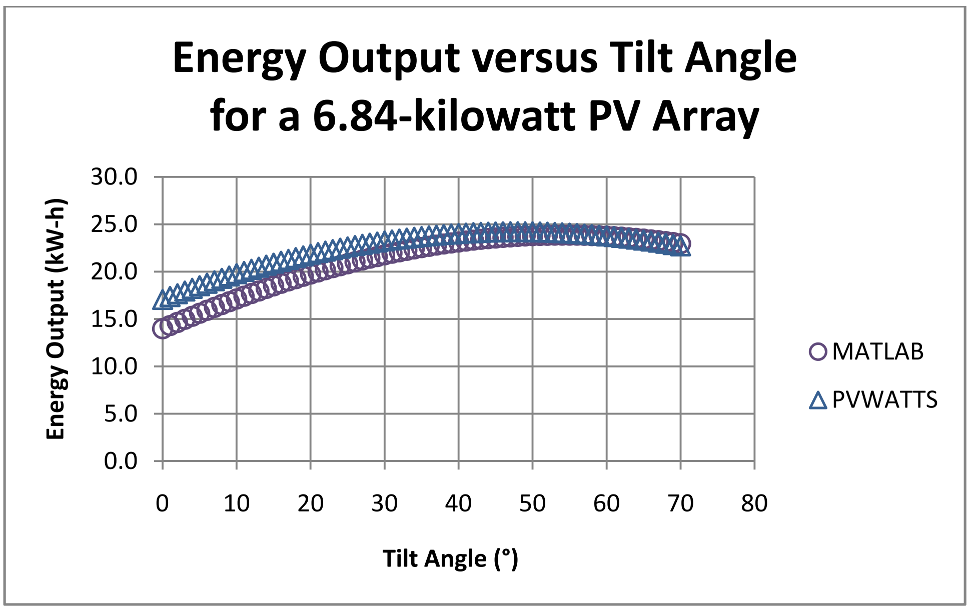

Figure 14: Comparison of MATLAB and PVWATTS results. The specified 6.84-kilowatt PV system comprises of 36 south-facing, monofacial, 190-watt PV modules in Washington, D.C. on October 12th, 2009.

Figure 14 demonstrates that the MATLAB and PVWATTS results are in reasonable agreement. While MATLAB shows the maximum energy output occurs at 54° tilt, PVWATTS shows that this peak occurs at 48° tilt. One reason for this difference is that only direct irradiance, and not diffuse irradiance, was considered in the MATLAB code. Another source of error stems from the way direct irradiance was approximated in MATLAB, by using a quadratic curve-fit. If a more accurate, normal distribution of irradiance versus time were used, the MATLAB results would perhaps have been in closer agreement with the PVWATTS results. Lastly, one other basis for this discrepancy is that PVWATTS calculates *monthly* energy production, though Figure 14 illustrates energy production for a single *day*. That is, in order to generate this plot it was assumed that energy production was uniform for all 31 days in October.

Despite these disparities, Figure 14 gives confidence that the analytical method exercised by MATLAB is essentially correct, and that the optimum tilt angle for the PV array is between 48° and 54°. With PVWATTS, the calculation process proved to be much faster than MATLAB. Additionally, PVWATTS incorporated a more accurate representation of incoming solar radiation which included both direct and diffuse components of irradiance. Thus, the PVWATTS calculator was the method of choice for estimating PV array performance.

4 Experimental Investigations

4.1 Test Stand Components

The experimental test stand was comprised of two 6-volt 50-mA Solar World solar cell modules (model number 4-6.0-50), an adjustable mounting structure, a Fluke Hydra Series II data logger (model number 2635A), and an Apogee pyranometer (model number SP-110). The components of the test stand are shown in Figure 15 and Figure 16.

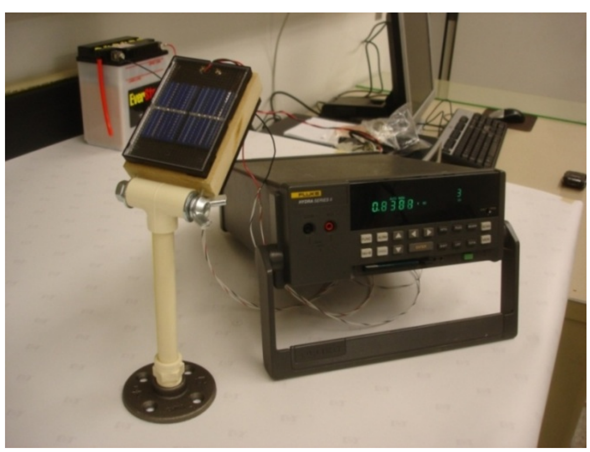

Figure 15: Photovoltaic modules, mounting structure, and data logger.

As shown in Figure 15, the two monofacial PV panels were mounted back-to-back to mimic the bifacial quality of a Sanyo Hit Double photovoltaic panel. The mounting structure allowed the lightweight PV panels to easily adjust to various heights and tilt angles. The data logger measured DC voltage output from the PV panels and pyranometer. The pyranometer sensor is shown in Figure 16.

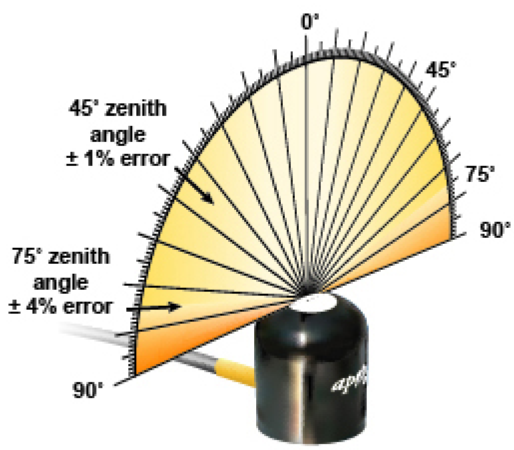

Figure 16: Apogee SP-110 pyranometer with 180° field of view (Apogee Instruments Inc., 2009).

As depicted in Figure 16, the pyranometer measures global irradiance or the sum of both direct and diffuse components of solar irradiance on a planar surface and with a 180° field of view. The transducer converts incident radiation to electrical current; and from the sensor's output voltage, insolation can be recorded. This particular sensor from Apogee is a silicon-cell photodiode pyranometer calibrated to measure shortwave radiation (Apogee Instruments Inc., 2009). Figure 17 shows the spectral response of the SP-110 Apogee pyranometer. Although the full spectrum for sunlight ranges from 280 to 2800 nanometers, nearly 90% of all solar energy is between 300 and 1100 nanometers (Apogee Instruments Inc., 2009). Thus, the Apogee SP-110 pyranometer is calibrated to measure this shortwave range of the sunlight spectrum.

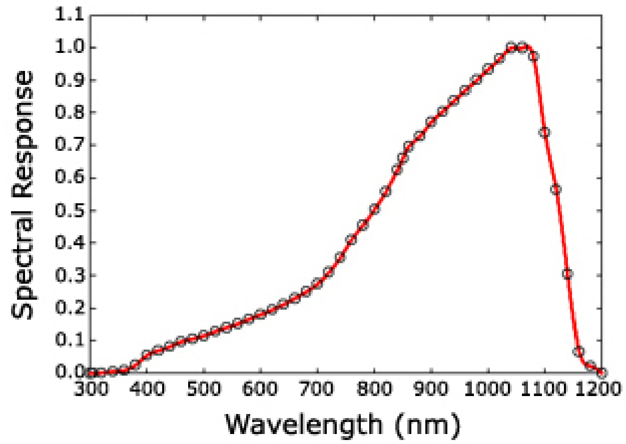

Figure 17: Spectral response of Apogee SP-110 pyranometer sensor (Apogee Instruments Inc., 2009).

4.2 Methodology for Experimental Analysis

The experimental investigations explored solar panel performance under actual, outdoor sunlight. Three tests were conducted to study various combinations of PV panel orientations and reflective surfaces. The first experiment examined how elevating the PV panels affected the total power output. The second experiment studied different reflectors, and how these reflective materials affected the power output of the back PV panel. The third experiment observed how power output differed when the PV panels were tilted at various angles.

In all three experiments, the pyranometer was kept stationary on the horizontal plane. Then, the amount of electrical power produced by the solar panels was weighed against the amount of solar radiation energy observed by the pyranometer, as shown by the following equation:

$$Percent\ Insolation\left[\%\right] = \frac{\left(\dfrac{Panel\ Power\ Output}{Panel\ Area}\right)\left[\dfrac{W}{m^2}\right]}{\left(Insolation\ on\ Horizontal\ Plane\right)\left[\dfrac{W}{m^2}\right]} \times 100\% \qquad \textbf{(5.1)}$$

In essence, the quantity “percent insolation” gauged the effectiveness of the PV panels, given the amount of insolation incident on the horizontal plane.

4.3 Elevation Test

The goal of the elevation experiment was to determine the optimum PV panel elevation at which the highest power output could be achieved. The experimental setup for the elevation test is shown in Figure 18.

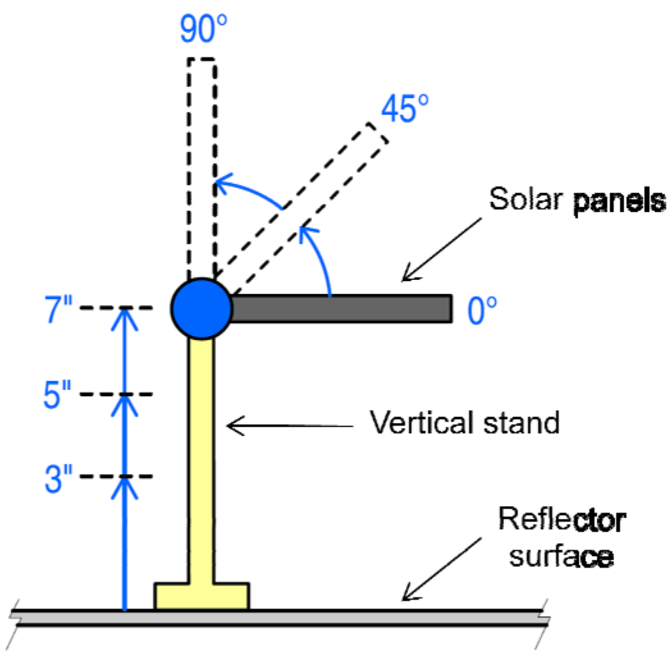

Figure 18: Setup for elevation test.

As illustrated in Figure 18, the PV panels were tested at three different elevations (3”, 5”, and 7”) as well as three different tilt angles (0°, 45°, 90°). The results of this elevation experiment are shown in Table 4.

Table 4: Results from elevation test, showing percent insolation at various elevations and tilt angles.

Percent Insolation (Averaged)				
Panel Face	Panel Tilt	Panel Elevation		
		7 inches	5 inches	3 inches
Front	90 °	2.75	5.68	5.75
Back		0.16	0.17	0.18
Front	45 °	5.81	5.89	5.85
Back		0.49	0.48	0.37
Front	0 °	5.84	5.97	5.96
Back		**0.83**	**0.75**	**0.42**

Table 4 shows that as panel tilt decreased, the percent insolation of the front panel increased. This was expected because the altitude angle of the sun was high during the time of data collection. However, Table 4 does reveal one anomalous data point, when the front PV panel face was tilted at 90° and elevated by 7 inches. At the time this data point was taken, it was observed that small electrical wires were obstructing a small portion of the front PV panel face. The resulting 2.75 percent insolation is quite low compared to measured front PV panel output from subsequent panel orientations. This obvious reduction in power output demonstrates the damaging effects of partially shading a solar panel.

The critical observation from the elevation experiment is seen on the bottom row of Table 4. Here, it is evident that the power output of the back face was significantly different at each of the three elevations. In comparing 3-, 7-, and 9-inch elevations, it was apparent that the 7-inch elevation was superior. This is a reasonable conclusion because at the 3-inch elevation, it was clear that the PV panel test stand directly shaded the reflector surface on the horizontal plane. Consequently, very little sunlight was being reflected to the PV panel back face.

Although an optimum panel elevation was not established, the findings from the elevation test suggest that raising the PV panel to a higher elevation was favorable. In addition, the largest disparity in power output was observed by the back PV panel when it was tilted at 0°. Therefore, the back PV panel was tilted at 0° in the subsequent reflector experiments, so as to examine clear differences in PV panel power output when different reflectors were applied.

4.4 Reflector Test

The goal of the reflector experiment was to determine the optimum PV panel elevation at which the highest power output could be achieved. The experimental setup for the reflector test is shown in Figure 19.

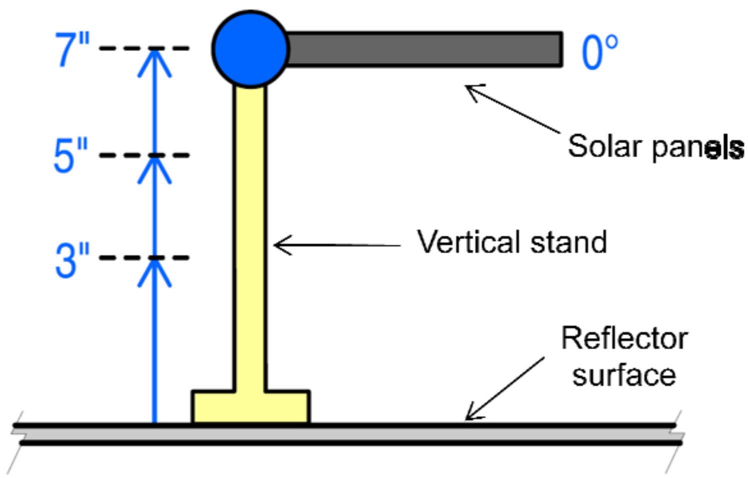

Figure 19: Setup for reflector test.

As illustrated in Figure 19, the PV panels were tested at 0° tilt and at three different elevations (3”, 5”, and 7”). The reflective surfaces were positioned on the horizontal plane. Combinations of mirror, white poster board, and textured acrylic sheets were investigated. The mirror (provided by Replex Plastics) was comprised of a flat sheet of acrylic with an aluminum coating. The textured acrylic, pictured in Figure 20, was an acrylic sheet with a prismatic, light-diffusing pattern (provided by Plaskolite, Inc.). This textured acrylic sheet with its prismatic pattern is commonly used for fluorescent office lighting fixtures.

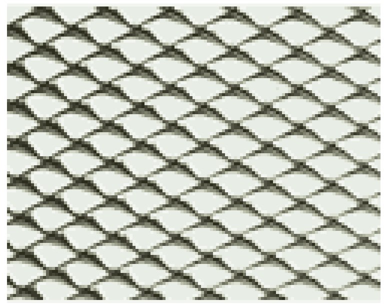

Figure 20: Textured acrylic sheet with prismatic pattern.

The textured acrylic sheet shown in Figure 20 was placed on top of the white poster board or on top of the mirror, in order to cause diffuse reflection. Altogether, the four reflector surfaces under investigation were: white poster board only, white poster board with textured acrylic top layer, mirror only, and mirror with textured acrylic top layer. For this experiment, the performance of the back PV panel face was of particular interest because the back face would primarily benefit from the reflectors. The results of the reflector experiment are shown in Table 5.

Table 5: Results from reflector experiments, showing percent insolation of the back PV panel face at various elevations and using various reflective surfaces.

Reflector Surface	Panel Elevation		
	7 inches	5 inches	3 inches
White Poster Only	**1.1**	**0.93**	**0.49**
White / Textured	1.02	0.83	0.37
Mirror / Textured	0.72	0.51	0.25
Mirror Only	0.73	0.12	0.06

Table 5 reveals that the reflector surface yielding the highest output, for the given time and day of data collection, was the unaccompanied white poster board. The data shows that the white poster board was superior for all three panel elevations. Due to the diffuse reflection of the white poster board, a large area of the white poster surface was directing low-intensity solar energy to the back PV panel. On the other hand, due to the specular reflection of the mirror, only a small area of the mirror surface was directing solar energy to the back panel face.

Although temperature was not monitored, another possible cause for the disparity in PV panel performance was heat. As mentioned before, solar panel efficiency decreases when temperature increases. One possible reason why the white poster board was superior was because the heat intensity of sunlight being reflected to the back PV panel face by the poster surface was lower than the heat intensity of sunlight reflected by the mirror surface. Further investigations would be needed to make any formal conclusions about the effects of temperature when different reflector surfaces are applied to the PV system.

4.5 Tilt Angle Test

The goal of this experiment was to determine the optimum PV panel tilt angle at which the highest power output is achieved. In an effort to support theoretical methods with experimental evidence, the results of this experiment were also compared to theoretical predictions. The experimental setup for the tilt angle test is shown in Figure 21.

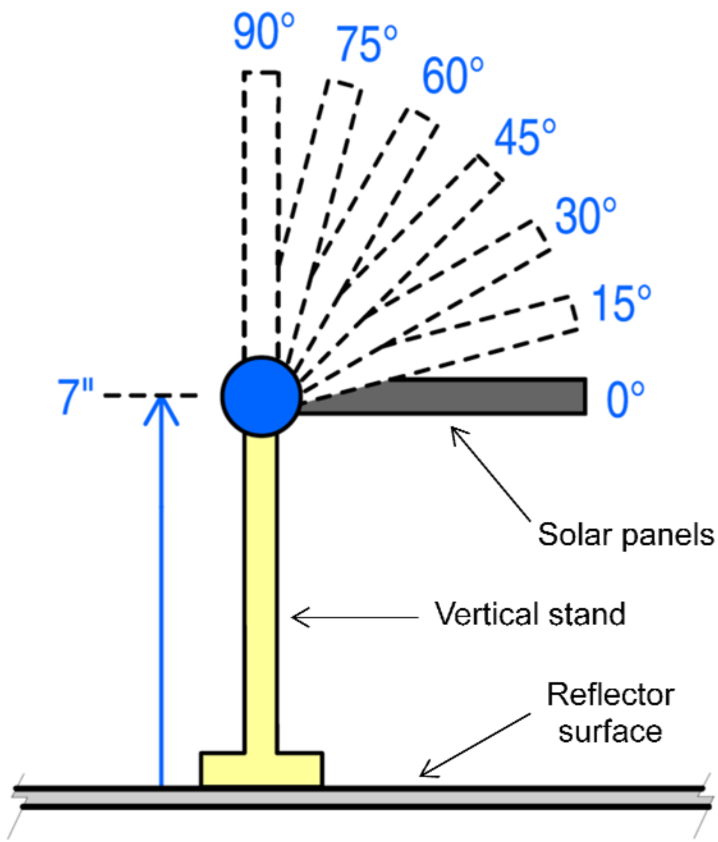

Figure 21: Setup for tilt angle test.

Since previous experiments showed that 7 inches was the best PV panel elevation and white poster board was the best reflector, these conditions were applied to the subsequent tilt angle test. As illustrated in Figure 21, the PV panels were tested at tilt angles ranging from 0° to 90° in increments of 15°. The tilting procedure was repeated for three different times of the day. The results of this experiment for times 11:00am, 1:30pm, and 4:30pm are shown in Figure 22, Figure 23, and Figure 24, respectively.

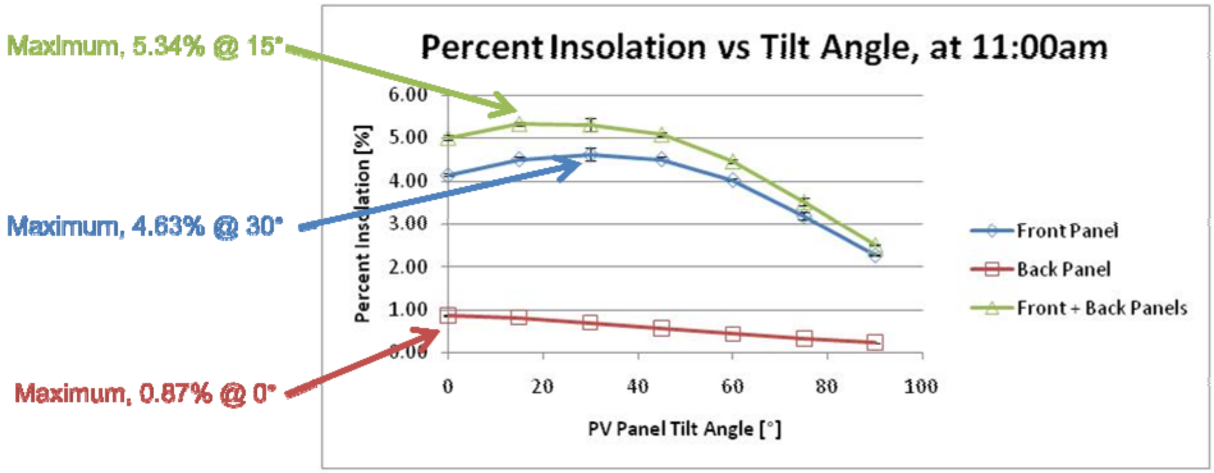

Figure 22: PV panel response for tilt angles ranging from 0° to 90°, at 11:00am.

Based on theoretical sun angles and experimentally measured insolation at 11:00am, the output of the front PV panel should peak at 40°. From Figure 22, the experimental data demonstrates that the front PV panel reached a maximum at 30°, which is in reasonable agreement with theory. The vertical error bars representing two standard deviations are minuscule, less than 0.15 percent insolation. This gives confidence that the measured PV panel output showed very small variations, and that the incoming solar radiation was fairly constant throughout the test.

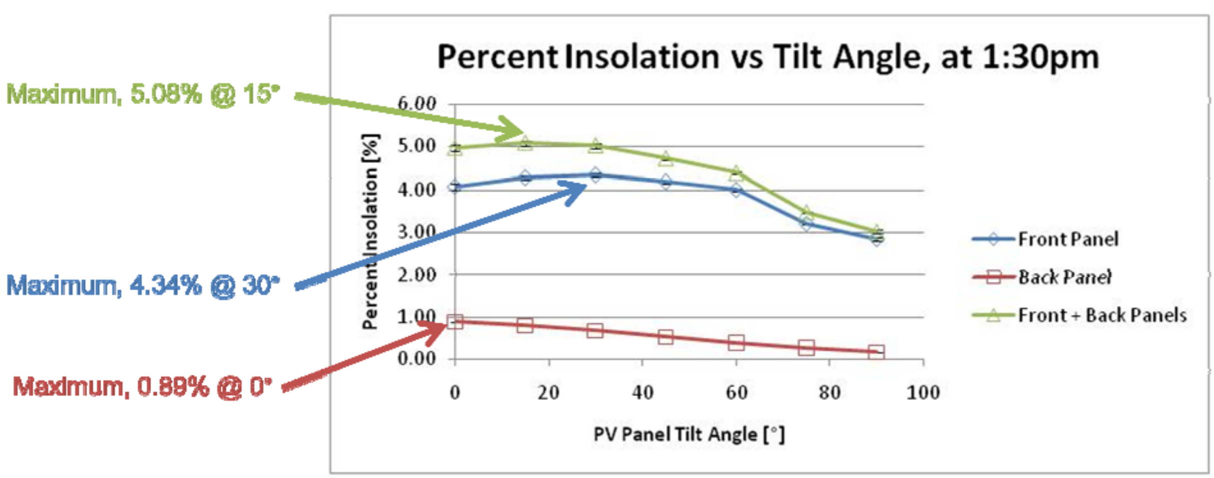

Figure 23: PV panel response for tilt angles ranging from 0° to 90°, at 1:30pm.

Based on theoretical sun angles and experimentally measured insolation at 1:30pm, the output of the front PV panel should peak at 27°. From Figure 23, the experimental data demonstrates that the front PV panel reached a maximum at 30°. Again, this is in reasonable agreement with theory. The vertical error bars representing two standard deviations are minuscule, less than 0.08 percent insolation. This gives confidence that the measured PV panel output showed very small variations, and that the incoming solar radiation was fairly constant throughout the test.

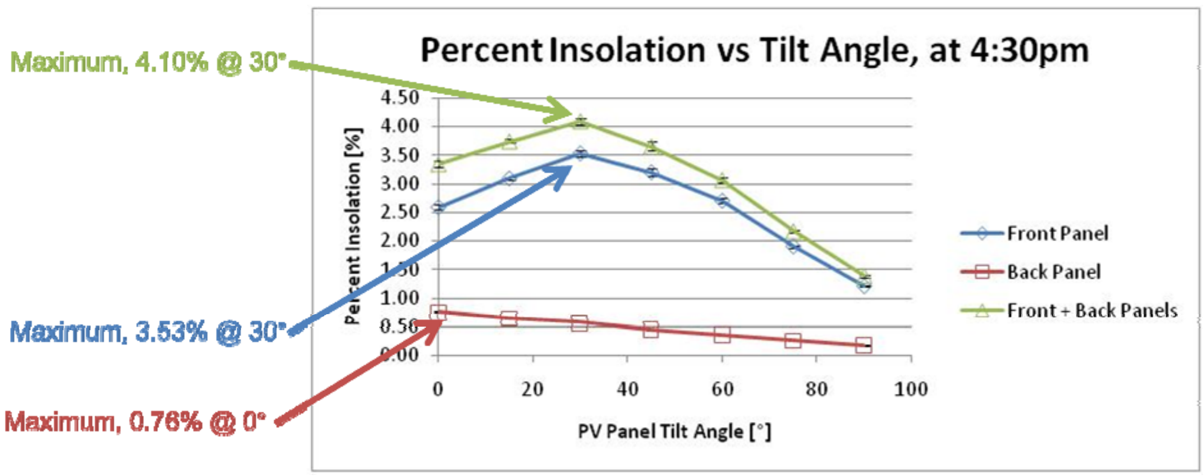

Figure 24: PV panel response for tilt angles ranging from 0° to 90°, at 4:30pm.

Based on theoretical sun angles and experimentally measured insolation at 4:30pm, the output of the front PV panel should peak at 50°. However, the experimentally determined peak shown in Figure 24 does not agree with theory. Experimentally, it was shown that the front PV panel reached a maximum at only 30°.

The data set obtained at 4:30pm not only differed from theoretical predictions but was also dissimilar to the responses at 11:00am and 1:30pm. One source of disparity was that the weather conditions at 4:30pm were windy, cloudy, shadowy, and visibly unlike the weather conditions of previous tests at 11:00am and 1:30pm. The increase in cloud cover at 4:30pm significantly decreased the power output and efficiency of the PV panels. Furthermore, with increased cloud cover the percentage of direct irradiance decreased, and diffuse irradiance increased. With increased diffuse irradiance, it makes sense that the optimum tilt angle would be lower, since aiming the front face of the PV panel directly toward the sun is of less importance. It is possible that laying the PV panel flat (parallel to the horizontal plane) would enhance the amount of diffuse irradiance striking the front face of the PV panel.

Unlike 11:00am and 1:30pm, the measured insolation at 4:30pm was unsteady throughout the duration of the test. Figure 25 shows the insolation measured by the pyranometer on the horizontal plane and illustrates the unevenness of incoming solar radiation energy, caused by the shifting cloud cover. The plot shows that at some moments during the test the insolation was relatively high, whereas at other moments the insolation was relatively low. The vertical error bars representing two standard deviations (±2σ = ±35.2 W/m2) further emphasizes the inconsistency of insolation throughout the duration of the 4:30 tilt angle experiment.

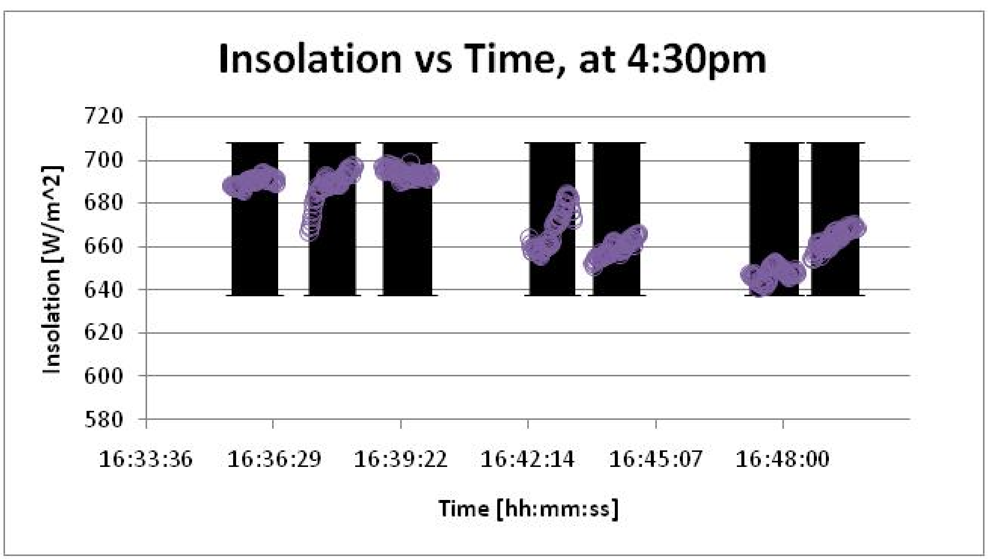

Figure 25: Insolation versus Time during tilt angle test, at 4:30pm.

Large moving clouds and adverse weather conditions in Washington, D.C. are potential challenges that may be encountered during the Solar Decathlon competition. The experimental findings from the tilt angle test demonstrate that the front PV panel performed as expected under ideal, sunny weather conditions; however the optimum tilt angle for the front PV panel was not in agreement with theory under cloudy weather conditions. These results underscore the reality that the performance of the rooftop PV array is heavily dependent on the weather and other environmental conditions during the week of competition.

4.6 Examining the Back Photovoltaic Panel

Drawing from the experimental results of the tilt angle test, a number of observations were made relating to the performance of the back PV panel. Figure 26, Figure 27, and Figure 28 show the back PV panel performance at 11:00am, 1:30pm, and 4:30pm, respectively.

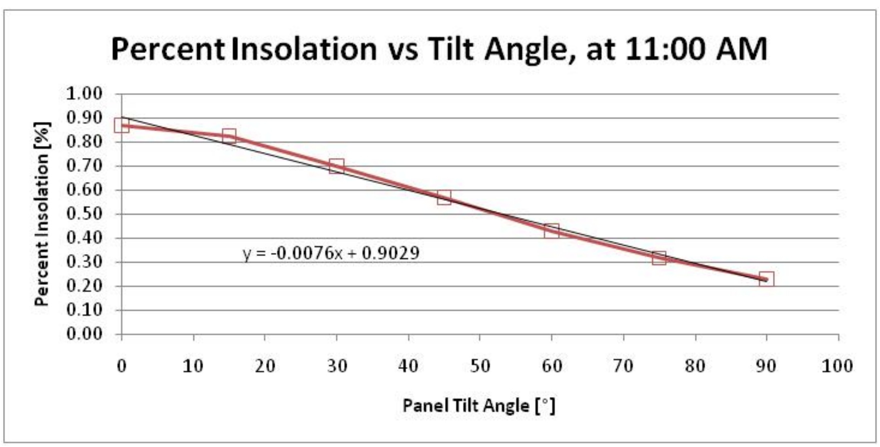

Figure 26: Back PV panel response for tilt angles ranging from 0° to 90°, at 11:00am.

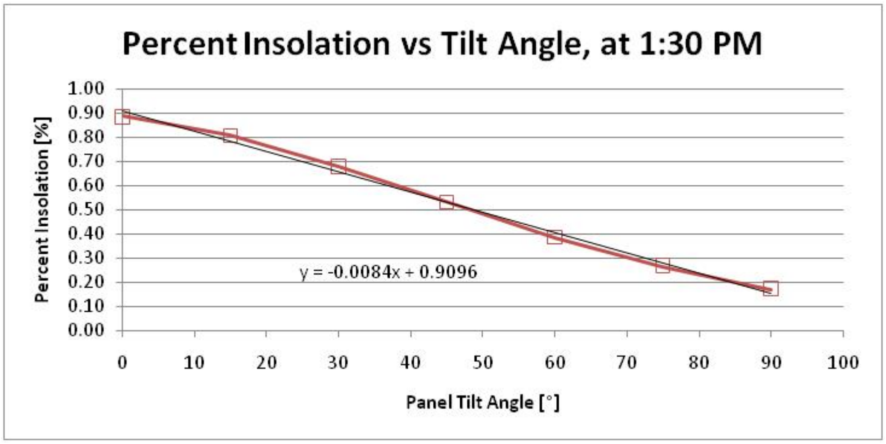

Figure 27: Back PV panel response for tilt angles ranging from 0° to 90°, at 1:30pm.

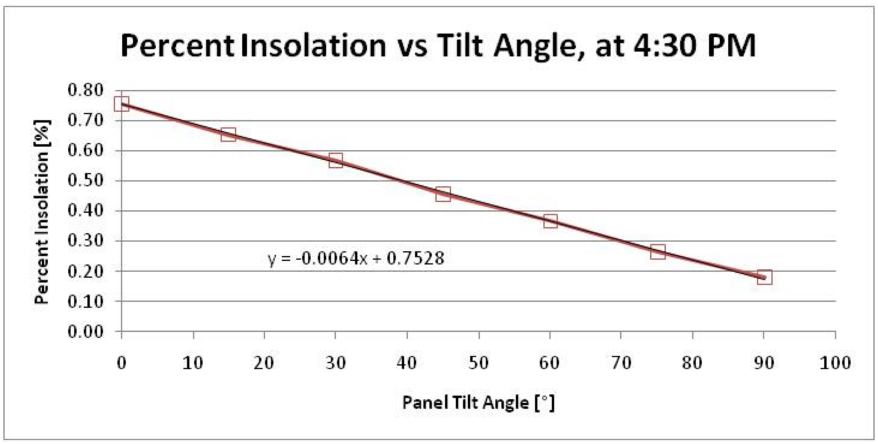

Figure 28: Back PV panel response for tilt angles ranging from 0° to 90°, at 4:30pm.

For all three cases, there exists a correlation between tilt angle and the efficiency of the back PV panel. Furthermore, the response is linear. This is an important observation because the power output of the back PV panel with respect to panel orientation was initially unknown. Given that there exists a linear relationship between back PV panel efficiency and tilt angle, a more accurate theoretical calculation could be performed in order to determine the optimum tilt angle for the rooftop PV array during the Solar Decathlon competition week. That is, this new calculation would account not only for the front face of the PV panel, but the back face as well.

An interesting subject for future research would be to observe whether or not this linear relationship remains true throughout an entire day. This could be accomplished by setting up multiple PV panel test stands at equal elevations and fixed at different tilts ranging from 0° to 90°. Then, measurements could be collected for a full day, from sunrise to sunset. From these test results, it would also be interesting to compare the front PV panel performance with theoretical predictions of PVWATTS performance calculator. If theoretical calculations for total energy output during one full day were supported by experimental evidence, then the PVWATTS program would earn further credibility. Consequently, this would give confidence to the 48° optimal tilt angle (for monofacial PV array in Washington, D.C. in October, 2009) that was computed during previous theoretical investigations.

5 Conclusions

Initial theoretical investigations computed the optimum tilt angle of the rooftop PV array for the 2009 OSU Solar Decathlon House. Analytical calculations incorporated the sun's position and irradiance at discrete instances of time throughout a single day. These results confirmed the theoretical results from the PVWATTS performance calculator, developed by the National Renewable Energy Laboratory (NREL). The optimum tilt angle for a south-facing, monofacial (one-sided) photovoltaic module in Washington, D.C. during October, 2009 was determined to be between 48° and 54°.

Experimental investigations demonstrated that a higher PV panel elevation was most favorable, in order to achieve higher power output from the back PV panel. This is a logical conclusion because when positioned at a lower elevation, the PV panel shaded the reflector surface underneath; consequently, the back PV panel face was scarcely illuminated.

Experimental investigations also revealed that a white poster board was the most favorable reflector surface, in order to achieve higher power output from the back PV panel. The white poster board diffusely scattered incoming sunlight, causing an even distribution of low-intensity solar radiation energy to illuminate the back PV panel face.

Under sunny, cloud-free weather conditions, it was demonstrated that experimental measurements of PV power output were in reasonable agreement with theory. That is, the measured optimum tilt angle for the front PV panel matched theoretical predictions. However, under cloudy weather conditions when the diffuse component of global irradiance was dominant, the experimental results did not correspond agreeably with theory and therefore the optimum tilt angle could not be predicted by analytical methods.

Lastly, the relationship between the efficiency and tilt angle of the back PV panel was linear. This linear response occurred at 11:00am, 1:30pm, and 4:30pm. Further investigation at all times of the day, from sunrise to sunset, is required to verify that this correlation exists continuously throughout the day. The findings from this analysis could help determine the optimum tilt angle for a bifacial (rather than a monofacial) photovoltaic module during the 2009 Solar Decathlon competition.

6 Recommendations for Future Work

One recommendation for future work would be to collect data continuously for an entire day, as opposed to distinct parts of one day. Multiple test stands could be used to investigate the power production from the front and back PV panels at varying tilt angles, ranging from 0° to 90°. Potentially, the findings from this experiment could accomplish three things:

1. Validate theoretical calculations for the energy output of the front PV panel.
2. Show that the relationship between efficiency and tilt of the back PV panel is linear for all times of the day.
3. Help determine the optimum tilt angle for a bifacial photovoltaic module during the 2009 Solar Decathlon competition.

Another recommendation for future work would be to examine how sunlight is reflected and absorbed by the mirror, poster, textured acrylic sheet, and other reflective surfaces. Also, temperature sensors could be used to monitor the intensity of sunlight being reflected from the reflector surface to the PV panels.

Finally, a third recommendation for future work would be to scale up the experimental results from the 6-volt solar panels, so as to compare them with the actual bifacial photovoltaic modules manufactured by Sanyo. If large discrepancies exist, then the small-scale test stand might be modified in order to better replicate the performance of the Sanyo Hit Double modules.

7 Acknowledgements

I would like to thank my advisor Dr. Mark Walter of the Department of Mechanical Engineering for his guidance and support. I thank Neil Gardner, Joe West, and Jerry Kingzett of the Mechanical Engineering machine shop and electronics lab for their assistance in building my experimental test stand. I would also like to thank Mark Schuetz and Mel Hazzard of Replex Plastics, as well as Dan Jones of Plaskolite, Inc. for providing the reflector materials that were examined in this research. Lastly, I would like to acknowledge the OSU Solar Decathlon Team for the outstanding work they have accomplished this past year.

8 Works Cited

Apogee Instruments Inc. (2009). *Pyranometer Technical Information*. Retrieved May 17, 2009, from Apogee Instrument Inc. Silicon-cell Photodiode Pyranometer: http://www.apogee-inst.com/pyranometer_techinfoSPECTRAL.htm

Autodesk, Inc. (2008). *Shading Design*. Retrieved May 17, 2009, from Autodesk Ecotect Environmental Building Design: http://squ1.org/wiki/Shading_Design

Hall, M., Roos, A., & Karlsson, B. (2005). Reflector Materials for Two-dimensional Low-concentrating Photovoltaic Systems: the Effect of Specular versus Diffuse Reflectance on the Module Efficiency. *Progress in Photovoltaics , 13* (3), 217-233.

Kyocera Solar, Inc. (2004). *Understanding Solar Electric Modules*. Retrieved May 15, 2009, from Kyocera Solar Energy Products: http://www.kyocerasolar.com/learn/modules.html

NASA. (2009). *NASA Surface Meteorology and Solar Energy*. Retrieved February 26, 2009, from Atmospheric Science Data Center: http://eosweb.larc.nasa.gov/cgi-bin/sse/grid.cgi?email=

National Renewable Energy Laboratory. (2008, July 25). *Renewable Energy Basics*. Retrieved May 17, 2009, from National Renewable Energy Laboratory: http://www.nrel.gov/learning/re_basics.html

NOAA. (2009). *NOAA ESRL Solar Position Calculator*. Retrieved April 24, 2009, from Earth System Research Laboratory: http://www.srrb.noaa.gov/highlights/sunrise/azel.html

NREL. (2009, April 6). *PV Watts Version 2 Calculator*. Retrieved 24 April, 2009, from National Renewable Energy Laboratory Renewable Resource Data Center: http://rredc.nrel.gov/solar/codes_algs/PVWATTS/version2/

Ronnelid, M., Karlson, B., Krohn, P., & Wennerberg, J. (2000). Booster Reflectors for PV Modules in Sweden. *Progress in Photovoltaics , 8* (3), 279-291.

Sanyo Electric Co. (2008, September 1). *Hit Double 190 Data Sheet.* Retrieved May 15, 2009, from Sanyo Solar Products: Hit Double Photovoltaic Modules: http://us.sanyo.com/HIT-Double/HIT-Double-Bifacial-Photovoltaic-Module

Sanyo Electric Co. (2009, January 1). *Hit Double General Installation Manual.* Retrieved May 15, 2009, from Sanyo Solar Products: Hit Double Photovoltaic Modules: http://us.sanyo.com/dynamic/product/Downloads/HIT%20Double%20Installation%20Manual%20(DA3)%2020090101-26232870.pdf

Sanyo Electric Co. (2008, September 1). *Hit Double Product Brochure.* Retrieved May 15, 2009, from Sanyo Solar Products: Hit Double Photovoltaic Modules: http://us.sanyo.com/dynamic/product/Downloads/HITDoublebrochure2008-30935473.pdf

U.S. Department of Energy. (2008, November 26). *About the Program*. Retrieved April 19, 2009, from U.S. Department of Energy: Solar Energy Technologies Program: http://www1.eere.energy.gov/solar/about.html

U.S. Department of Energy. (2008, October 1). *Contests and Scoring*. Retrieved May 7, 2009, from Solar Decathlon: http://www.solardecathlon.org/contests_scoring.html

U.S. Department of Energy. (2008, May 22). *Light and the PV Cell*. Retrieved May 17, 2009, from U.S. Department of Energy: Solar Energy Technologies: http://www1.eere.energy.gov/solar/pv_cell_light.html

Wikipedia. (2009, April 15). *Insolation*. Retrieved May 17, 2009, from Wikipedia: The Free Encyclopedia: http://en.wikipedia.org/wiki/Insolation

Wikipedia. (2009, April 7). *Solar Power in Germany*. Retrieved May 17, 2009, from Wikipedia: The Free Encyclopedia: http://en.wikipedia.org/wiki/Solar_power_in_Germany

9 Appendices

9.1 Sanyo Hit Double 190 Data Sheet

Think GAIA
For Life and the Earth

SANYO

Bifacial Photovoltaic Module

HIT Double190
Photovoltaic Module

Power per Square Foot up to 18.6 Watts

High Efficiency

HIT® Double bifacial solar panels are the World leaders in sunlight conversion efficiency, helping customers to enjoy the maximum power per square foot from available space.

Power Guarantee

SANYO guarantees customers will receive 100% of the panel's rated power (or more) at the time of purchase, enabling owners to generate more kWh per rated watt.

Bifacial Effect

The back face of HIT Double solar panels generates electricity from ambient light reflected off surrounding surfaces, and combines with power from the front face of the panel. Dependant upon system design and site albedo, this results in up to 30% higher power generation (more kWh) per square foot.

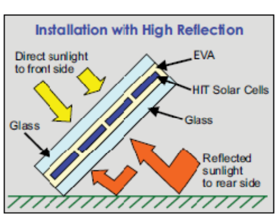

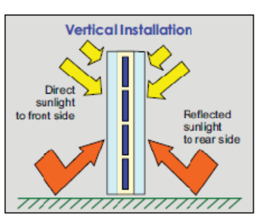

Application Possibilities

- Architectural, Awnings, Balconies, Bus Shelters, BIPV
- Deck & Porch Coverings, Canopies, Carports, Facades
- Fences, Siding, Trellises, Tracking Systems

Proprietary Technology

HIT bifacial solar cells are hybrids of single crystalline silicon surrounded by ultra-thin amorphous silicon layers, available solely from SANYO.

High Temperature Performance

As temperatures rise, HIT Double solar panels produce more electricity than conventional solar panels at the same temperature, for good performance in high temperature sites.

Quality Products

SANYO silicon wafers are made in California USA, and assembled in Mexico at SANYO's certified factory. ISO 9001 (quality), 14001 (environment), 18001 (safety).

Valuable Features

HIT Double panels operate silently and have no moving parts. A double glass structure allows some sunlight to penetrate portions of the panel, creating brilliant light and shadows for aesthetic and architectural applications. HIT Double panels are perfect for areas with performance-based incentives and tradable energy credits.

HIT Double 190
Photovoltaic Module

Electrical Specifications

Model: HIP-190DA3	STC[1]	5%	10%	15%	20%	25%	30%
		Specifications Including Backside Irradiation Contribution in ISC as a Percent of STC					
Rated Power (Pmax)[1]	190 W	199 W	208 W	216 W	225 W	234 W	243 W
Maximum Power Voltage (Vpm)	55.3 V	55.30 V	55.36 V	55.42 V	55.50 V	55.52 V	55.56 V
Maximum Power Current (Ipm)	3.44 A	3.60 A	3.75 A	3.91 A	4.06 A	4.22 A	4.37 A
Open Circuit Voltage (Voc)	68.1 V	68.3 V	68.4 V	68.5 V	68.6 V	68.6 V	68.8 V
Short Circuit Current (Isc)	3.7 A	3.89 A	4.07 A	4.26 A	4.44 A	4.63 A	4.81 A
Max. System Voltage (Vsys)	600 V	—	—	—	—	—	—
Series Fuse Rating	15 A	—	—	—	—	—	—
Temperature Coefficient (Pmax)	-0.3% / °C	—	—	—	—	—	—
Temperature Coefficient (Voc)	-0.170 V / °C	—	—	—	—	—	—
Temperature Coefficient (Isc)	0.85 mA / °C	—	—	—	—	—	—
Warranted Tolerance	+10/-0%	—	—	—	—	—	—
Cell Efficiency	18.8%	—	—	—	—	—	—
Module Efficiency[2]	15.7%	16.4%	17.1%	17.8%	18.6%	19.3%	20.0%
Power per Square Foot	14.6 W	15.2 W	15.9 W	16.6 W	17.2 W	17.9 W	18.6 W

Mechanical Specifications

Internal Bypass Diodes	4 Bypass Diodes
Module Area	13.06 Ft² (1.21 m²)
Module Weight	50.7 Lbs. (23 kg)
Module Dimensions LxWxH	53.2 x 35.35 x 2.36 in. (1351 x 898 x 60 mm)
Cable Lengths	39.4 in. each (1000 mm)
Cable Size / Connector Type	No. 12 AWG / MC3™ Connectors
Static Load	50 PSF (2400 Pa)
Pallet Dimensions LxWxH	54.3 x 36 x 70.1 in. (1379 x 912 x 1781 mm)
Full Pallet Quantity & Weight	20 pcs. / 1014 Lbs. (460 kg)
Quantity per 20'/40'/53' Container	200 pcs., 420 pcs., 540 pcs.

Safety Ratings & Limited Warranty

Fire Safety Classification	Class A
Hail Safety Impact Velocity	1" hailstone (25 mm) at 52 mph (23 m/s)
NOCT (°C)	115.8°F (46.6°C)
Safety & Rating Certifications	UL 1703, cUL, CEC
Limited Warranties	2 Years Workmanship / 20 Years Power Output

[1]Standard Test Conditions: Cell Temperature 25°C, Air Mass 1.5, 1000 W/m²
[2]Equivalent module efficiency, including power from the back face.
Note: Specifications and information above may change without notice.

Dimensions Unit: inches (mm)

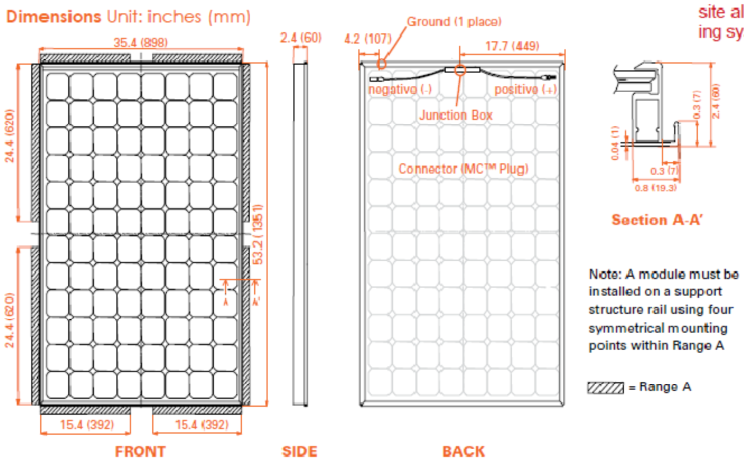

To Maximize Power

1. Elevate panels above a surface as much as possible.
2. Place panels over light-colored surfaces.
3. Do not allow support rails to shade the panel's back face.

Dependence on Temperature

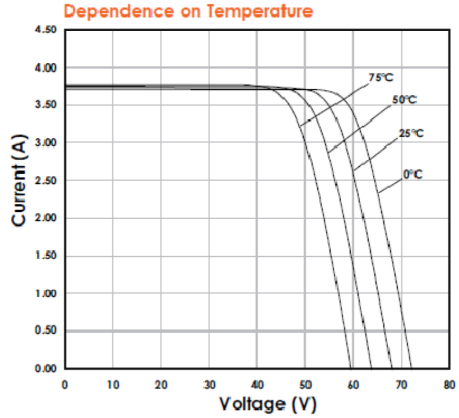

Dependence on Irradiance

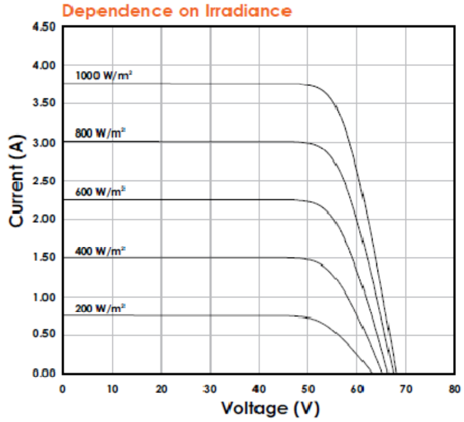

IMPORTANT: The rated power of HIT® Double bifacial solar panels is measured under Standard Test Conditions (STC). STC does not account for power produced from the back face of panels. Therefore, HIT Double panels will produce more power than their STC rating, up to 30% more, depending upon the system design and site albedo. Account for the additional power when sizing, selecting system components and wiring.

CAUTION! Read the operating instructions carefully before use of these products

SANYO

SANYO Energy (U.S.A.) Corp.
Solar Division

2600 Network Blvd., Suite 600
Frisco, TX 75034, U.S.A.
www.sanyo.com/solar
solar@sec.sanyo.com

9.2 Theoretical Analysis, MATLAB Code

```
% ME 581 - written by Raymond Dong - 1/22/2009

clc; clear all; close all; format long;

% -------------------- SOLAR ANGLES --------------------

% Read sun angle data from Excel spreadsheet "SunData.xlsx".
time        = xlsread('SunData.xlsx', 'Oct12', 'C11:C58'); % minutes
altitude    = xlsread('SunData.xlsx', 'Oct12', 'D11:D58'); % degrees
azimuth     = xlsread('SunData.xlsx', 'Oct12', 'E11:E58'); % degrees

% -------------------- SOLAR INSOLATION --------------------

% Define three points on the solar insolation curve (sunrise, solar noon,
% and sunset).
yINSOLATION = xlsread('SunData.xlsx', 'Oct12', 'I11:I13') % kW/(m^2)
xTIME       = xlsread('SunData.xlsx', 'Oct12', 'H11:H13') % minutes

% Fit quadratic curve for pseudo insolation curve.
pfit = polyfit(xTIME,yINSOLATION,2);         % polynomial coefficients
pval = polyval(pfit,xTIME(1):1:xTIME(3));                  % kW/(m^2)
insolation = (pfit(1)*time.^2+pfit(2)*time+pfit(3));       % kW/(m^2)

% Plot insolation versus time of day.
figure(1)
plot(xTIME(1):1:xTIME(3),pval,'r-',time,insolation,'o','Linewidth',2);
grid on;
title('Insolation versus Time of day')
xlabel('Time (minutes)')
ylabel('Insolation (kW/m^2)')
legend('Quadratic curve','Insolation data',1)

% Incorporate panel efficiency.
efficiency = 0.157;                                        % unitless
insolation = insolation*efficiency;                        % kW/(in^2)

% Incorporate inverter efficiency.
efficiency = 0.94;                                         % unitless
insolation = insolation*efficiency;                        % kW/(in^2)

% Define range of panel angles to analyze.
min_angle = 0;    % degrees
max_angle = 90;   % degrees

for (i = min_angle:1:max_angle)
    % NOTE:  Panel angle is the variable to be optimized.
    panel       = i;                        % degrees
    phi         = 90 - altitude - panel;    % degrees

    % --------------------  DIRECT SOLAR INSOLATION --------------------
```

```
    % Magnitude of direct insolation projected in the direction FROM true
    % south TO true north.
    D1 = insolation.*cos(azimuth*pi/180);     % kW/(in^2)

    % Magnitude of direct insolation projected to line perpendicular to
    % face of PV panel.
    D2 = D1.*cos(phi*pi/180);               % kW/(in^2)

    % --------------------  POWER & ENERGY --------------------

    % Calculate power by multiplying incident direct solar insolation by
    % area of individual panel.
    area = 1.21;        % m^2
    power = D2*area;    % kW

    % Calculate total energy per day by integrating power.
    energy(i+1) = trapz(time,power)/(60);   %kW-hr

    if i == 54;
        % Plot power output versus time of day
        figure(i+1)
        plot(time,power,'bo','LineWidth',2);
        grid on;
        title('Single Panel Output Power versus Time of Day')
        xlabel('Time (minutes)')
        ylabel('Power (kW)')
    end

    % Display results for energy ouput to the command window.
    fprintf('Daily energy produced by single solar panel at %f degrees is %f
kW-hr\n', i, energy(i+1))
end

% Display best and worst values for energy output to the command window.
BEST = max(energy);     % kW-hr
WORST = min(energy);    % kW-hr
fprintf('\nBEST energy produced by solar array is %f kW-hr\n', BEST)
fprintf('WORST energy produced by solar array is %f kW-hr\n', WORST)

% Plot energy output versus panel angle.
figure(max_angle+2)
plot(min_angle:1:max_angle,energy,'b-','LineWidth',2);
grid on;
title('Daily Energy Output for Single Panel at Varying Panel Tilt Angles')
xlabel('Panel angle (degrees)')
ylabel('Energy output (kW-hr)')

% Write results to Excel spreadsheet entitled "ResultsData.xls".
ANGLES = [min_angle:1:max_angle]';      % degrees
xlswrite('ResultsData.xls', ANGLES, 'Energy Output', 'A2');
xlswrite('ResultsData.xls', energy', 'Energy Output', 'B2');
```